Crossed-Slot Antenna Array Design for an Incoherent Scatter Radar and Characteristic Modes Analysis

Juan Pablo Ciafardini [(1)], Eva Antonino Daviu [(2)], Marta Cabedo Fabrés [(2)], Nora Mohamed Mohamed-Hicho [(2)], J. Alberto Bava [(1)], Miguel Ferrando Bataller [(2)].
[(1)] Dpto. de Electrotecnia. Facultad de Ingeniería, Universidad Nacional de La Plata. Calle 48 y 116 - La Plata (1900), Argentina. jpciafardini@fcaglp.unlp.edu.ar
[(2)]Instituto de Telecomunicaciones y Aplicaciones Multimedia. Edificio 8G. Planta 4ª, acceso D. Universidad Politécnica Valencia. Camino de Vera, s/n46022 Valencia. España. evanda@upvnet.upv.es

***Abstract*—This paper describes the design and construction of a crossed slot antenna array to be applied to an Incoherent Scatter Radar for measuring parameters of the Ionosphere. The slot antenna was designed and optimized with electromagnetic simulation software. An analysis of the characteristic modes of the elementary antenna of the array is performed, in order to obtain a physical understanding of the radiating behavior. A prototype of a linear crossed-slot antenna array has been constructed and measured, as an intermediate step for the development of a two-dimensional array.**

***Index Terms*—slot antenna, antenna array, Characterictics Modes , Incoherent Sacatter Radar.**

I. INTRODUCTION

One of the tools developed to study the ionosphere is the Incoherent Scatter Radar, which can measure a wide range of ionospheric parameters and provide information about the properties and behavior of the neutral atmosphere in general [1],[2].

The current state of technology allows the development of such radar by adopting the concept of antenna array; avoiding the use of mechanical aiming systems and enabling instant changes of the beam direction modify its radiation pattern and generate multiple beams. Examples of these radars are the AMISR (Advanced Modular Incoherent Scatter Radar) [3], [4], and the EISCAT 3D (European incoherent scattering radar), which is currently being developed in Scandinavia [5].

This paper describes the design of a linear array antenna as an intermediate step for further bidimensional arrangements, intended to be applied in incoherent scatter radar. The basic element of the array is a crossed-slot antenna designed to operate at 432 MHz frequency with circular polarization, which should enable the reverse polarization. A characteristic mode analysis of the basic element will be performed in order to get more physical insight into the radiating behavior of the element. The antennas were designed using electromagnetic simulation software (FEKO 7.0 and CST Microwave Studio Suite 2014). Graphs of the measurements made on the constructed models are shown and compared with the results obtained by simulations.

II. CROSSED-SLOT ANTENNA

The elementary antennas used in Ionospheric Radar based in antenna arrays are, in general, crossed dipoles type or Crossed Yaguis [6], [7].

The antenna developed in this work [8], as an elemental antenna of an ionospheric Radar group, is a slot type antenna (crossed-slot antenna), designed to operate in the range between 430 and 434 MHz. It consists of two orthogonal slots carved on a metal plate with a flat reflector at the rear. The geometry of the antenna is shown in Fig. 1. The slots are directly fed into the center by an unbalanced line [9], [10]. An outline of the crossed-slot antenna is shown in Fig. 2. As observed, one port is connected between terminals A and B and the other between terminals C and D. The length of the antenna side is L = 450 mm, and the slots have a length of 558 mm and a width of 10 mm.

Fig. 1. Crossed-Slot Antenna Prototype.

In order to achieve circular polarization, the two slots are fed with a phase shift of 90°. By reversing the relative phase shift between the slots, right circular polarization or left circular polarization is obtained. This is one of the requirements of ionospheric radar.

III. Analysis of Characteristic Modes of a Crossed-Slot Antenna

The Theory of Characteristic Modes has demonstrated to be really helpful for the analysis and design of different types of antennas. The success of Characteristic Modes lies on the physical insight they provide, especially when they are used for understanding the radiating behavior of metallic structures of simple geometry in which currents flow following predictable schemes [11].

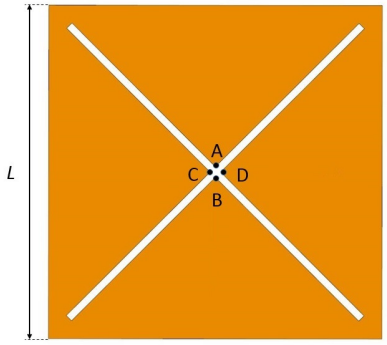

Fig. 2. Crossed-Slot Antenna.

Characteristic modes (J_n) are real current modes that are extracted at every frequency from the generalized impedance matrix of the antenna. This matrix is obtained by the direct application of Method of Moments. This way, characteristic modes correspond with the eigencurrents of the matrix, and therefore they depend only on the shape and size of the antenna. As characteristic modes form a set of orthogonal functions, they can be used to expand the total current on the surface of the antenna as follows:

$$J = \sum_n \frac{V_n^i J_n}{1 + j\lambda_n} \tag{1}$$

Where J_n are the eigencurrents, λ_n are the eigenvalues and V_n^i is the modal excitation coefficient.

The modal excitation coefficient can be obtained as:

$$V_n^i = \left\langle J_n, E^i \right\rangle = \iint_S J_n \cdot E^i dS \tag{2}$$

Consequently, the product in $V_n^i J_n$ in (1) models the coupling between the excitation and the n^{th} mode, and determines which modes will be excited. Extensive explanation of how to compute eigencurrents J_n and eigenvalues λ_n of a conducting body is given in [12].

Once the basics of the theory of characteristic modes have been reviewed, let us perform a modal analysis of the antenna structure shown in Fig. 2. Fig. 3 shows the normalized current distribution at first resonance for the first five characteristic modes, J_n, of the antenna. Red arrows have been plotted together with characteristic currents for a better understanding of the current flow. Mode J_0 is a non-resonant mode, whereas modes J_1 and J_1' are degenerated modes (that resonate at the same frequency), due to the symmetry of the structure. Note that modes J_2 and J_2' are not degenerate modes.

The resonance frequency and radiating bandwidth of the above described current modes can be obtained from the information yield by characteristic angles. Characteristic angles (α_n) can be computed from eigenvalues (λ_n) as:

$$\alpha_n = 180° - \tan^{-1}(\lambda_n) \tag{3}$$

Physically, a characteristic angle models the phase difference between a characteristic current J_n and its associated characteristic field E_n [11].

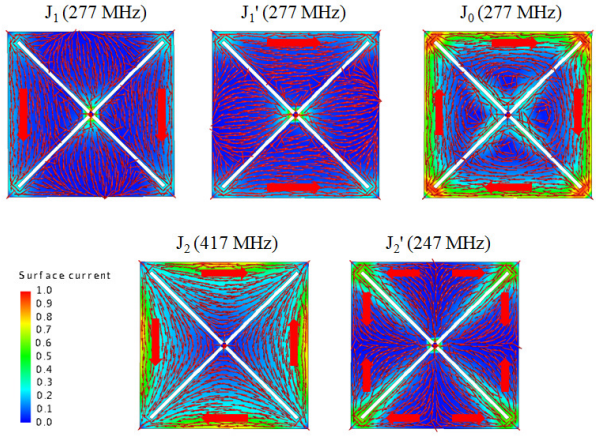

Fig. 3. Normalized current distribution of the first five characteristic modes of the crossed-slot antenna.

At the resonance frequency, this phase difference is 180º. Therefore, when characteristic angle is close to 180º the mode is a good radiator, while when characteristic angle is near 90º or 270º the mode mainly stores energy. This means that the radiating bandwidth of a mode can be obtained from the slope near 180º of the curve described by characteristic angles.

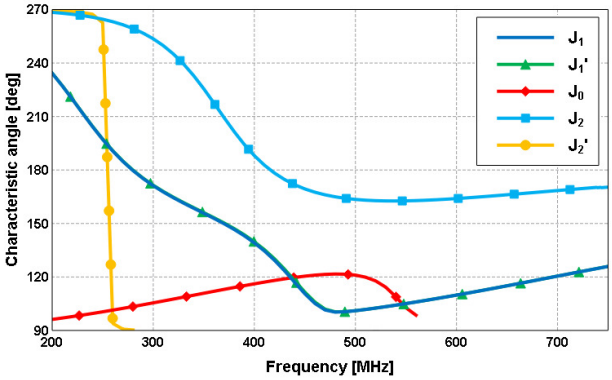

Fig. 4. Characteristic angle versus frequency for the first five modes of the crossed-slot antenna.

The modes J_1 and J_1' are modes of the square ground plane. In a square ground plane without slots, the resonance of J_1 and J_1' modes occurs when the side length is approximately $L = \lambda/2$. In the case of the crossed slots antenna, the resonance frequency of these modes is shifted down due to the effect of the slots that force the currents to follow a longer electrical path. Mode J_2 is also a mode of the ground plane. Its resonance is not affected because the location of the slots in the ground plane does not affect the current distribution corresponding to this mode. The presence of the slots produces an additional resonant mode in the structure, the J_2' mode called slot mode. As observed in Fig. 4, the curve of the characteristic angle associated to this mode presents a very steep slope, what entails a narrowband behavior for this mode. Slot mode resonates when the electrical length of the external perimeter is approximately λ. When excited, this slot mode interacts with the modes of the planar structure and creates an impedance mismatch that results in a band notch effect [13].

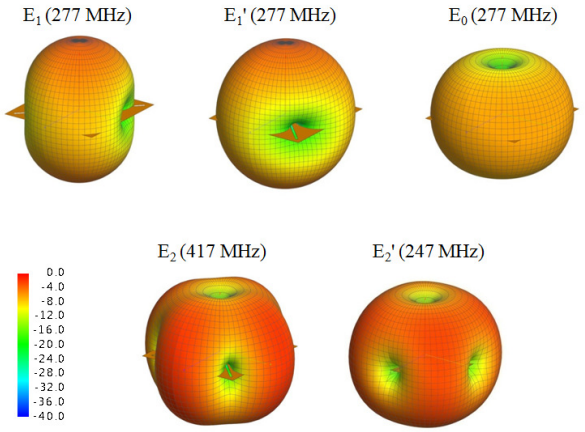

Fig. 5. Normalized characteristic electric fields of the first five modes of the crossed-slot antenna.

Finally, Fig. 5 shows the normalized characteristic electric fields (E_n) associated to the characteristic currents of Fig. 3. These modal far field patterns and characteristics currents have been obtained with FEKO [14] by using Characteristic Modes request.

Now we perform an analysis of the excitation of the characteristic modes. Either inductive or capacitive coupling mechanisms can be used to excite characteristic modes. In general terms, inductive feeding will effectively excite those modes whose electric current distribution shows a maximum at the location of the source. The larger the magnitude of the modal electric current distribution is at the source position, the more the mode will be excited. On the contrary, capacitive coupling mechanism will effectively excite those modes where the electric field shows a maximum at the source location.

In the case of the feed given to the crossed slots antenna, described above, only the modes J_1, J_1' and J_2' can be excited effectively since only these modes have a maximum current at the feed point, as seen in Fig. 3. Connecting a voltage source between points A and B of Fig. 1, J_1 mode can be fed, and connecting a voltage source between points C and D, J_1' mode can be excited. Mode J_2' may be feed by performing a combination of both voltage sources, however if we make an impedance matching analysis, we could see that mode J_2' cannot be feed properly.

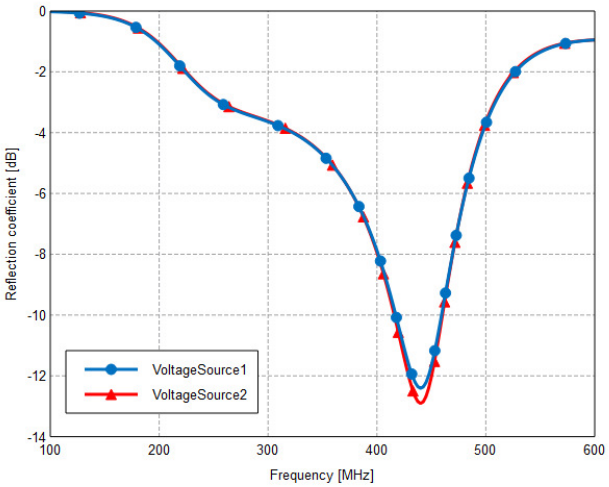

Fig. 6. Simulated reflection coefficient for the feeding ports of the slots.

Fig. 6 depicts the simulated reflection coefficient for each port of the crossed slot antenna. As observed, a bandwidth from 410 to 460 MHz is obtained for S_{11}< -10 dB. In this frequency range, J_1 and J_1' modes have a characteristic angle of about 120º (see Fig. 4), acting as radiating modes. However, the characteristic angle of J_2' mode is 90º, behaving as energy storage mode.

In Fig.7 a), normalized radiation pattern of the crossed slot antenna obtained by feeding the two antenna ports at frequency of 432 MHz is shown. It can be seen that the pattern obtained is a combination of the normalized characteristic electric fields E_1 and E_1', shown in Fig. 5.

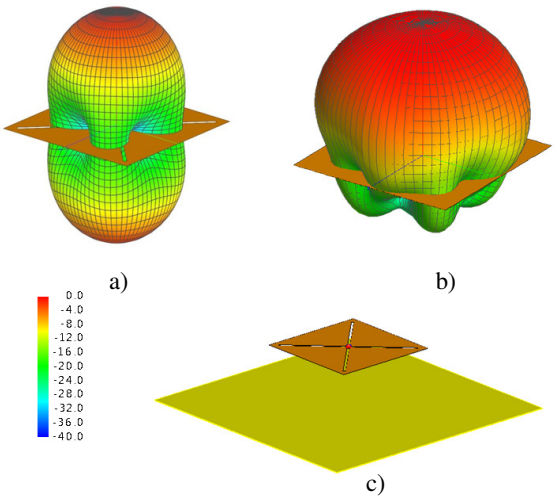

Fig. 7. Normalized radiation patterns obtained from simulations: a) Crossed-Slot Antenna, b) Crossed-Slot Antenna with ground plane reflector. c) Model of the Crossed-Slot Antenna with ground plane reflector used for simulations.

If degenerated modes J_1 and J_1' are fed with a phase shift of 90º, circular polarization is obtained. Moreover, in order to make the antenna radiate only upward, a rectangular ground plane separated approximately λ/4 is placed, as shown in Fig. 7 c). The resulting radiation pattern is shown in Fig. 7 b).

The separation between the antenna and the ground plane was optimized with FEKO 7.0 software [14] in order to achieve high cross-polarization rejection. Results are shown in Fig. 8.

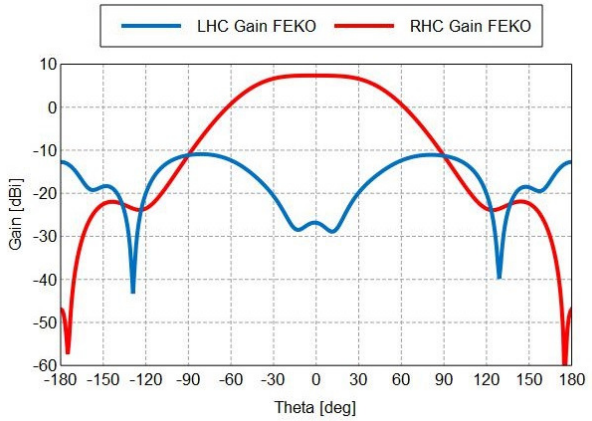

Fig. 8. Radiation pattern obtained from simulations of the crossed-slot antenna. Co-polar component in red and cross-polar component in blue.

IV. Linear Crossed Slot Antenna Array

A linear array [15] was designed based on the crossed-slot antenna, with the main objective to achieve the displacement of the main beam to ± 30 ° from the central position, avoiding significant degradation in the main lobe to lobe side. For this purpose four antennas forming a rectilinear cross linear array with constant spacing between centers of 0.65 λ antenna slots are arranged. In order to feed radiators, uniform current distribution was used. A scheme of the implementation of the grouping is shown in Fig. 10. The progressive angle ($\Delta\varphi$), which is required to achieve the displacement of the main beam generated by the grouping, can be calculated using (4), where σ is the angle desired for the main beam, d is the distance between centers of radiating elements, and λ is the free space wavelength.

$$\Delta\varphi = \frac{360° \times d \times sen\ \sigma}{\lambda} \qquad (4)$$

TABLE I. Displacement of the antenna beam angle vs. progressive angle of each antenna

Displacement of the antenna beam angle σ	0°	10°	20°	30°
Progressive Angle Δφ	0°	40.6°	80°	120.6°

Progressive values of phase angle shifts required to achieve the main beam of 0 °, 10 °, 20 ° and 30 ° are shown in Table 1.

In Fig. 9 the results obtained by software simulation considering an infinite flat metal plane as reflector are shown. In Fig. 9 a) the Cartesian plot corresponding to angles 0º, 10º, 20º and 30º is presented, whereas in Fig. 9 b) the 3D radiation patterns obtained for displacements of the main beam at the same angles are shown. It stresses that main lobe related to side lobes is ≥8dB for all shifting of the main beam.

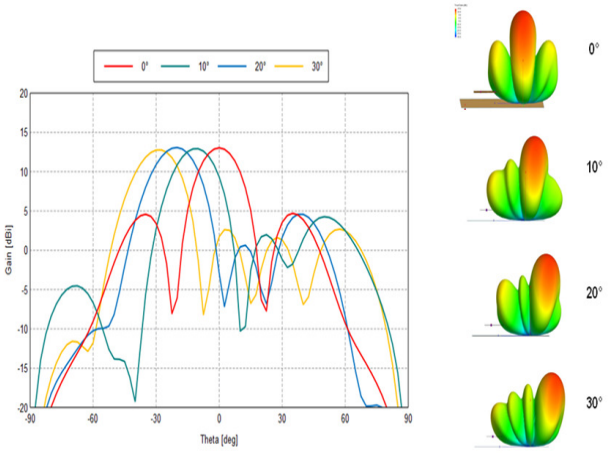

a) b)

Fig. 9. Results obtained by software simulation for displacements of the main beam in angles of 0º, 10º, 20º and 30º. a) Cartesian diagram corresponding to each angle; b) 3D radiation diagrams.

V. Measurements

The proposed linear antenna array (shown in Fig. 10) was fabricated and measured, comparing the results with those obtained by simulation. The linear array was built in a metal sheet where the slots were carved. A reflector consisting of a thin metal mesh was located under the array and the entire structure was mounted on a prepared support.

Fig. 10. Linear antennas array built with four crossed slot antennas.

The antenna is excited by a power divider that divides the input signal into four signals of equal phase and amplitude. Each of these signals is injected into a shifter which controls the relative phase of the signals feeding each antenna. The shifter used is a design that employs a 90º hybrid coupler and varactor diodes. This configuration allows a phase shift between 0° and 360º [16].

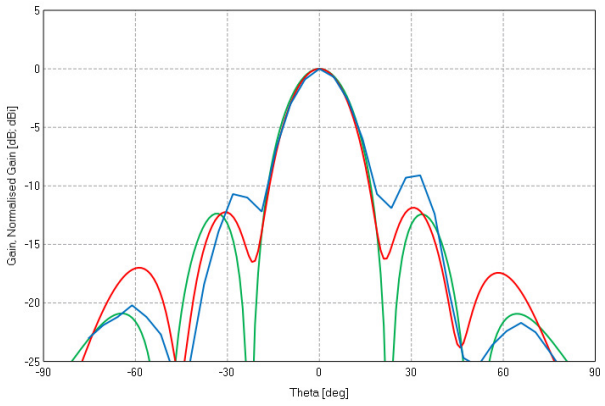

a)

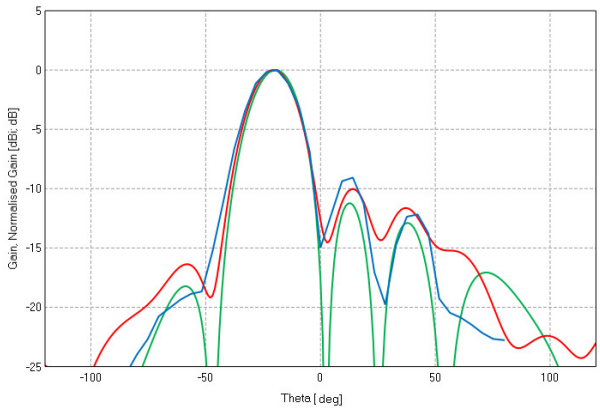

b)

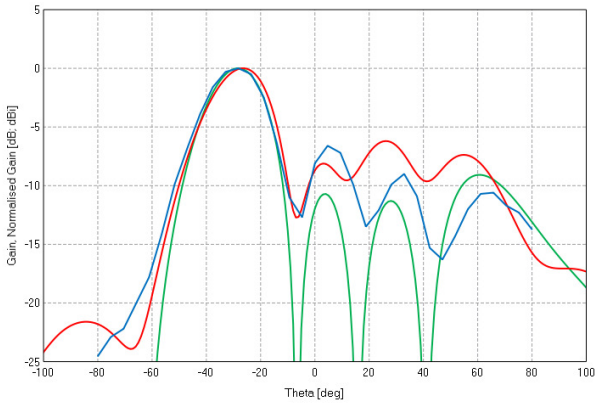

c)

Fig. 11.Results obtained from measurements and simulation of the radiation pattern of the linear array prototype for the displacement of the main beam of: a) 0°, b) 20º and c) 30º.

Measurements of the radiation pattern of the antenna array for displacement angles of the main beam of 0°, 20° and 30° are shown in Fig. 11 (in blue color), overlapped with simulated results with FEKO 7.0 (red curve) and CST (green curve). As observed, measured and simulated results are in good agreement.

VI. Conclusions

The results of the measurements meet the requirements and are consistent with the obtained results using software simulations performed during the design stages. It should be noted that measurements of the radiation patterns were performed in open space, due to the large dimensions of the antenna. More accurate measurements should be performed in an appropriate environment (anechoic chamber) with low noise rejection. Also polarization measurements should be carried out.

For a complete evaluation of the design, one possibility is to re-scale the antenna array for operating at higher frequencies, in order to obtain an array with smaller dimensions.

References

[1] Hargreaves, J. K., (1995). "The solar – terrestrial environment". *Cambridge Atmospheric and Space Sciences Series.*

[2] Hunsucker, R. D., (1991). "Radio Techniques for Probing the Terrestrial Ionosphere*". Physics and chemistry in space; v. 22. Springer-Verlag. Berlin Heidelberg 1991.*

[3] Valentic, T., Buonocore, J., Cousins, M., Heinselman, C., Jorgensen, J., Kelly, J., Malone, M., Nicolls, M., Van Eyken, A., (2013). "AMISR the Advanced Modular Incoherent Scatter Radar". *Phased Array Systems & Technology, 2013 IEEE International Symposium on.*

[4] Bob Robinson. "The Advanced Modular Incoherent Scatter Radar (AMISR), Historical Perspectives". *National Science Foundation.*

[5] EISCAT 3D description and status. (2015).

[6] ESICAT 3D Final Design Study Report. (2009).

[7] Hysell, D.L.;Cornell Univ., Ithaca, NY, USA; Chau, J.L.; Milla, M.A.(2013)."TheJicamarcaphased-arrayradar". *PhasedArraySystems&Technology, 2013 IEEE International Symposiumon.*

[8] Ciafardini, J. P., Garcia, E., Rodriguez, G., Bava, J. A., (2014). "Antena de ranuras cruzadas para un radar ionosférico*". BiennialCongress of Argentina (ARGENCON). IEEE.*

[9] Kraus, J. D., (1998). "Antennas*". Mcgraw Hill.*

[10] Knorr, J. B., (1974). "Slot-Line Transitions". *IEEE Transactions on microwave theory and techniques, MAY 1974.*

[11] M. Cabedo-Fabrés, E. Antonino-Daviu, A. Valero-Nogueira, and M. Ferrando-Bataller, "The Theory of Characteristic Modes Revisited: A Contribution to the Design of Antennas for Modern Applications," *IEEE Trans. Antennas Propagat. October 2007.*

[12] R. F. Harrington and J. R. Mautz, "Theory of characteristic modes for conducting bodies," *IEEE Trans. Antennas Propagat., vol. AP-19,pp. 622-628, Sept. 1971.*

[13] E. Antonino-Daviu, M. Cabedo-Fabres, M. Ferrando-Bataller, and V.M. Rodrigo-Peñarrocha, "Modal analysis and design of band-notched UWB planar monopole antennas" *IEEE Trans. Antennas Propagat. , vol. 58, no. 5, pp. 1457–1467, May 2010.*

[14] EM Software & Systems - S.A. (Pty) Ltd - FEKO (www.feko.info) - *EM Software & Systems - S.A. (Pty) Ltd Address: PO Box 1354, Stellenbosch, 7599, South Africa.*

[15] Ángel Cardama Aznar, Lluís Jofre Roca, Juan Manuel RiusCasals, Jordi Romeu Robert, Sebastián Blanch Boris, Miguel Ferrando Bataller, (2002). "Antenas". *Edicions de la UniversitatPolitècnica de Catalunya, SL.*

[16] Rodriguez, Guillermo D.; Garcia, Ricardo E.; Ciafardini, Juan P., (2014) "Desplazador de fase para un radar ionosférico" *Biennial Congress of Argentina (ARGENCON). IEEE.*

[17] CST Microwave Studio Suite 2014, CST Inc., 2014.